HHS Public Access

Author manuscript

ACS Nano. Author manuscript; available in PMC 2021 March 24.

Published in final edited form as:

ACS Nano. 2020 March 24; 14(3): 3378–3388. doi:10.1021/acsnano.9b09263.

Nanoparticle-Mediated Co-Delivery of Notch-1 Antibodies and ABT-737 as a Potent Treatment Strategy for Triple-Negative Breast Cancer

Danielle M. Valcourt, **Megan N. Dang**, **Mackenzie A. Scully**

Department of Biomedical Engineering, University of Delaware, Newark, Delaware 19716, United States

Emily S. Day

Department of Biomedical Engineering and Department of Materials Science and Engineering, University of Delaware, Newark, Delaware 19716, United States; Helen F. Graham Cancer Center and Research Institute, Newark, Delaware 19713, United States

Abstract

Triple-negative breast cancer (TNBC) accounts for nearly one-quarter of all breast cancer cases, but effective targeted therapies for this disease remain elusive because TNBC cells lack expression of the three most common receptors seen on other subtypes of breast cancer. Here, we exploit TNBC cells' overexpression of Notch-1 receptors and Bcl-2 anti-apoptotic proteins to provide an effective targeted therapy. Prior studies have shown that the small molecule drug ABT-737, which inhibits Bcl-2 to reinstate apoptotic signaling, is a promising candidate for TNBC therapy. However, ABT-737 is poorly soluble in aqueous conditions, and its orally bioavailable derivative causes severe thrombocytopenia. To enable targeted delivery of ABT-737 to TNBC and enhance its therapeutic efficacy, we encapsulated the drug in poly (lactic-co-glycolic acid) nanoparticles (NPs) that were functionalized with Notch-1 antibodies to produce N1-ABT-NPs. The antibodies in this NP platform enable both TNBC cell-specific binding and suppression of Notch signaling within TNBC cells by locking the Notch-1 receptors in a ligand unresponsive state. This Notch inhibition potentiates the effect of ABT-737 by up-regulating Noxa, resulting in effective killing of TNBC cells. We present the results of *in vitro* studies that demonstrate N1-ABT-NPs can preferentially bind TNBC cells *versus* noncancerous breast epithelial cells to effectively regulate Bcl-2 and Notch signaling to induce cell death. Further, we show that N1-ABT-NPs can accumulate in subcutaneous TNBC xenograft tumors in mice following systemic administration to reduce tumor burden and extend animal survival. Together, these findings demonstrate that NP-

Corresponding Author: Emily S. Day – Department of Biomedical Engineering and Department of Materials Science and Engineering, University of Delaware, Newark, Delaware 19716, United States; Helen F. Graham Cancer Center and Research Institute, Newark, Delaware 19713, United States; emilyday@udel.edu.

Supporting Information

The Supporting Information is available free of charge at https://pubs.acs.org/doi/10.1021/acsnano.9b09263.

DLS and ζ potential of NPs in serum, Notch-1 immunocytochemistry staining, light microscopy images of NP interaction with MCF-10A cells, average tumor diameter throughout *in vivo* therapeutic study, mouse weight throughout *in vivo* therapeutic study, H&E staining of major organs, primer sequences for qRT-PCR (PDF)

Complete contact information is available at: https://pubs.acs.org/10.1021/acsnano.9b09263

The authors declare no competing financial interest.

mediated co-delivery of Notch-1 antibodies and ABT-737 is a potent treatment strategy for TNBC that may improve patient outcomes with further development and implementation.

Graphical Abstract

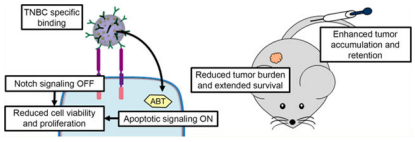

Keywords

gene regulation; drug delivery; multivalency; Notch signaling; nanocarrier; signal cascade interference; targeted cancer nanomedicine

Triple-negative breast cancer (TNBC) is an aggressive disease that accounts for 15–25% of all breast cancer cases, yet it lacks effective treatment strategies.[1,2] As its name implies, TNBC does not express the three most common receptors found on other subtypes of breast cancer: estrogen receptor, progesterone receptor, and human epidermal growth factor receptor 2. This characteristic lack of expression leaves TNBC unsusceptible to current targeted or hormonal therapies, thus resulting in high mortality and recurrence rates.[1–3] Here we exploited TNBC cells' overexpression of Bcl-2 anti-apoptotic proteins and Notch-1 receptors to develop an effective targeted therapy.[4–8]

The p53 apoptotic pathway is activated in healthy cells when they experience external stress or DNA damage.[2] Upon activation, acetylated p53 migrates to the mitochondria where it induces Bax-mediated release of cytochrome c. Cytochrome c then stimulates a series of caspase activations that ultimately promote apoptosis in the cell.[9] In TNBC, however, the pro-survival protein Bcl-2 is overexpressed, and this amplification is associated with poor prognosis.[10,11] Bcl-2 binds to Bax, suppressing cytochrome c release from the mitochondria to prevent initiation of apoptosis[9,12] (Scheme 1a). Thus, inhibiting Bcl-2 to promote apoptosis is a promising alternative strategy to combat TNBC.[6]

Several methods to inhibit Bcl-2 are in development, and some of these use Bcl-2 homology 3 (BH3) mimetics to bind Bcl-2 directly.[13–15] One such BH3 mimetic, ABT-737, has been shown to potently induce apoptosis in cancer cells characterized by dysregulated p53 signaling by reinstating Bax-mediated release of cytochrome c.[13–17] However, ABT-737 has poor aqueous solubility and has therefore only been delivered orally in the clinic. Unfortunately, orally delivered ABT-737 has poor bioavailability, so it has not been explored further in clinical trials.[18] An orally bioavailable derivative of ABT-737, Navitoclax (ABT-263), has also been explored in the clinic, but it causes severe thrombocytopenia.[19–21] Effective strategies for ABT-737 delivery to targeted tumors are needed to allow this drug to realize its clinical potential.

To improve the solubility and bioavailability of ABT-737, two different research teams have encapsulated the drug in nanoparticles (NPs).[16,22] Schmid *et al.* showed that encapsulating ABT-737 in PEGylated polymeric NPs could reduce the thrombocytopenia associated with

delivery of the free drug.[16] They also coencapsulated a topoisomerase I inhibitor, camptothecin, to achieve synergistic apoptosis in *in vitro* and *in vivo* colorectal cancer models.[16] Jin and colleagues similarly coencapsulated ABT-737 and an IRAK1/4 inhibitor in PEG-modified poly(lactic-co-glycolic acid) (PLGA) NPs to synergistically treat T cell acute lymphoblastic leukemia (T-ALL).[22] They demonstrated that IRAK/ABT-NPs could effectively induce an apoptotic T-ALL fraction at a concentration 2-fold lower than the free drug combination *in vitro* and significantly restore white blood cell numbers in the peripheral blood of a T-ALL mouse model.[22] The demonstration that these two NP formulations could effectively mitigate the side effects of ABT-737 while maintaining its potency prompted us to develop a NP platform for targeted delivery of ABT-737 to TNBC. In designing this platform, we desired not only to provide targeted delivery of ABT-737 to TNBC cells but also to combat resistance to ABT-737 that is present in TNBC cells and driven by Notch signaling.

Recent studies in a variety of cancers have shown that aberrant activation of Notch signaling contributes to cellular resistance to ABT-737.[15,17,23] In brief, the Notch signaling pathway is activated in cancer cells when Jagged/Delta ligands on signal sending cells interact with Notch receptors on signal receiving cells. This leads to a sequence of two cleavages of the Notch transmembrane receptor by ADAM 10/17 and the γ-secretase complex, with the Notch intracellular domain (NICD) ultimately translocating to the nucleus where it promotes the expression of several downstream oncogenes (Scheme 1a).[24] Gamma secretase inhibitors are a class of drugs that prevent the second of the Notch receptor cleavage events, thus inhibiting downstream activity in the Notch signaling pathway.[17] When Notch signaling is suppressed, a protein called Noxa that is associated with overcoming resistance to ABT-737 is upregulated. Noxa displaces the Bcl family proteins Bcl-B, Bfl-1, and Mcl-1 from Bax, thus reinstating downstream apoptotic signaling. Accordingly, by combining Notch inhibitors with ABT-737, apoptosis induction is enhanced.[13,17,23] Given that Notch signaling is elevated in TNBC[8,25] and that combining Notch inhibitors with Bcl-2 inhibitors has shown promise in other cancers, we aimed to develop NPs that could enable targeted treatment of TNBC while simultaneously exploiting this dual therapeutic strategy.

In this work, we coated ABT-737-loaded PLGA NPs with Notch-1 antibodies to produce N1-ABT-NPs that enable TNBC cell-specific drug delivery and simultaneous inhibition of Notch signaling (Scheme 1b). Notch-1 receptors are overexpressed on the surface of TNBC cells[8,25] and thus provide a handle for NP attachment that helps retain the NPs in the tumor microenvironment.[26] Further, upon binding TNBC cells, the N1-ABT-NPs can block Notch-1 receptor interactions with Jagged/Delta ligands on neighboring cells to suppress Notch signaling. Notably, our group and others have shown that antibody-coated NPs exhibit multivalent binding that leads to enhanced signal cascade interference relative to freely delivered antibodies.[27,28] Thus, by functionalizing our NP formulation with Notch-1 antibodies, we can enable Notch signaling inhibition to potentiate the effect of ABT-737 while simultaneously providing targeted drug delivery. Here, we demonstrate that N1-ABT-NPs regulate Bcl-2 and Notch signaling to enhance cell death *in vitro* and reduce tumor burden *in vivo*, warranting their further investigation for treatment of TNBC and other cancers that are characterized by aberrant Bcl-2 and Notch signaling.

RESULTS AND DISCUSSION

Characterization of Antibody and Drug Loading in N1-ABT-NPs.

N1-ABT-NPs synthesized as depicted in Figure 1a and described in the Methods were characterized using dynamic light scattering (DLS), ζ potential, absorbance, and enzyme-linked immunosorbent assay (ELISA) measurements, which demonstrated that antibodies were successfully conjugated to the surface of ABT-737-loaded NPs. Before antibody conjugation, ABT-737-loaded NPs had a hydrodynamic diameter of 52.8 ± 0.9 nm and a surface charge of −41.3 ± 5.6 mV, with 48 μg ABT-737 encapsulated per 1 mg of PLGA (Figure 1b,c). To put this in perspective, empty NPs have a size and ζ potential of 48.4 ± 4.5 nm and −14.4 ± 1.2 mV, respectively. Upon conjugation of IgG or Notch-1 antibodies, the ABT-737-loaded NPs' hydrodynamic diameter increased by approximately 20 nm and the ζ potential approached neutral, indicating successful antibody attachment (Figure 1b). During antibody conjugation, about 50% of the encapsulated ABT-737 is lost, leaving 23–26 μg drug encapsulated per mg PLGA (Figure 1c). This suggests some of the drug may have been adsorbed to the surface of the NPs rather than encapsulated. We further evaluated the release of ABT-737 from the NPs in storage (4 °C in water) and physiological conditions (37 °C in phosphate buffered saline (PBS)) over a 3 day period using absorbance values of the lyophilized drug no longer encapsulated in the NPs. After 72 h in storage conditions, <15% of the ABT-737 was released from N1-ABT-NPs. At 37 °C in PBS, however, up to 55% was released within the same 72 h time period (Figure 1d).

We also examined the stability of N1-ABT-NPs in 0%, 10%, 50%, and 100% fetal bovine serum (FBS) over a 24 h period. The hydrodynamic diameter (Figure S1a) and ζ potential (Figure S1b) of these NPs remained relatively stable at serum concentrations up to 50%. When incubated in 50% and 100% FBS over 24 h, the size and surface charge of these NPs notably increased, indicating a substantial protein corona accumulates on the particles at these higher serum concentrations. Altogether, these data demonstrate ABT-737 can be successfully loaded inside antibody-functionalized NPs that are stable in serum and will release the therapeutic cargo upon exposure to physiological conditions.

Notch-1 Antibody Functionalization Enables Preferential NP Interaction with TNBC Cells.

Next, we evaluated how Notch-1 and IgG antibody-functionalized NPs interacted with MDA-MB-231 TNBC cells that overexpress the Notch-1 receptor (Figure S2a) and with healthy MCF-10A mammary epithelial cells that have low Notch-1 receptor expression (Figure S2a). For these studies, the NPs were loaded with DiD fluorophores to enable their detection by fluorescence microscopy and flow cytometry. We treated cells with IgG-DiD-NPs or N1-DiD-NPs at 80 nM DiD for 4 h, after which DiD was only detected in MDA-MB-231 TNBC cells by fluorescence microscopy when delivered *via* Notch-1 functionalized NPs (Figure 2a). IgG-DiD-NPs showed minimal interaction with either MDA-MB-231 cells (Figure 2a) or MCF-10A cells (Figure S2b), and N1-DiD-NPs demonstrated low levels of interaction with MCF-10A cells that lack Notch-1 receptor overexpression (Figure S2b). We further analyzed NP interaction with both cell types using flow cytometry after treating cells for 1, 4, 8, 12, 16, or 24 h. At each time point, N1-DiD-NPs showed enhanced interaction with MDA-MB-231 TNBC cells relative to IgG-DiD-NPs, and this interaction was time

dependent (Figure 2b,c). After 24 h, MDA-MB-231 cells treated with N1-DiD-NPs exhibited a 3-fold higher median fluorescence intensity than cells treated with IgG-DiD-NPs. The fluorescence intensity of MCF-10A cells treated with N1-DiD-NPs was similar to the background levels observed for MDA-MB-231 cells treated with IgG-DiD-NPs, indicating minimal interaction between N1-DiD-NPs and MCF-10A cells (Figure 2c). Overall, these data indicate that Notch-1 antibody functionalization provides enhanced and specific NP interaction with MDA-MB-231 TNBC cells.

N1-ABT-NPs Induce TNBC Cell Death and Reduce Proliferation *in Vitro*.

To determine if Notch-1 antibody-functionalized NPs can potentiate the effect of ABT-737 against TNBC cells, we examined the relative metabolic activity of MDA-MB-231 cells treated with free ABT-737 and IgG or Notch-1 antibodies or with nanocarriers of the drug and antibodies. After a 72 h treatment period, 3-(4,5-dimethylthiazol-2-yl)-2,5-diphenyltetrazolium bromide (MTT) assays showed that, when freely delivered in combination with either IgG antibodies or Notch-1 antibodies, the IC_{50} of ABT-737 is approximately 2.6 μM (Figure 3a). When encapsulated in IgG-functionalized NPs, the IC_{50} remains in the same range as the freely delivered components, at a value of 3.2 μM. By comparison, when delivered *via* N1-ABT-NPs, the IC_{50} drops notably to 1.6 μM (Figure 3a). This demonstrates that using a nanocarrier to co-deliver Notch-1 antibodies and ABT-737 to TNBC cells is advantageous *versus* delivering the molecules freely in solution. Further, it supports the conclusions of prior studies that show Notch inhibitors can potentiate the effects of ABT-737.

We further evaluated the impact of N1-ABT-NPs on TNBC cell function using an EdU proliferation assay. We treated cells with NPs at a dose corresponding to 3 μM ABT-737 and 0.9 μg/mL antibodies for 72 h. The EdU assay results demonstrate that IgG-ABT-NPs cause a mild reduction in cell proliferation, but N1-ABT-NPs significantly reduce the percentage of proliferative cells by 46% (Figure 3b, representative histograms in Figure 3c). This corroborates the MTT data that indicate that Notch-1 functionalized, ABT-737-loaded NPs can potently suppress TNBC cell viability and proliferation.

N1-ABT-NPs Regulate Bcl-2 and Notch Signaling in TNBC Cells.

To determine whether the enhanced therapeutic effect seen with N1-ABT-NPs is simply due to increased drug delivery or also a result of Notch signaling interference mediated by the antibodies (Figure 4a), we evaluated the expression of Bcl-2 and Notch signaling targets in TNBC cells treated with N1-ABT-NPs or IgG-ABT-NPs using qRT-PCR and Western blotting. qRT-PCR shows that IgG-ABT-NPs reduce Bcl-2 mRNA expression by 59%, but have no significant effect on the expression of Noxa, Hes5, or HeyL, which are regulated by Notch signaling. This indicates that ABT-737 is successfully released from IgG-ABT-NPs to reduce Bcl-2 mRNA expression. N1-ABT-NPs expectedly knocked down Bcl-2 expression by 61%, but also reduced Hes5 expression by 42% and HeyL expression by 38%, and increased Noxa expression 2.4-fold (Figure 4b). Western blot analysis revealed similar results, as N1-ABT-NPs suppressed Bcl-2 (17%) and Hes1 (72%) protein expression, while IgG-ABT-NPs did not suppress these proteins (Figure 4c, representative bands in Figure 4d). We also probed for cleaved Notch-1, but did not observe a significant change in the

expression of this protein. Altogether, the qRT-PCR and Western blot data confirm that N1-ABT-NPs can both inhibit Bcl-2 and effectively regulate the Notch signaling pathway.

Notch-1 Functionalization Enhances NP Tumor Accumulation and Retention *in Vivo*.

After validating N1-ABT-NPs could inhibit TNBC cell viability through the expected molecular mechanisms *in vitro*, we next evaluated their ability to reduce tumor burden *in vivo* using a subcutaneous murine xenograft model. First, we investigated the tumor accumulation and retention of DiD-loaded NPs after intravenous injection into female nude mice bearing subcutaneous MDA-MB-231 tumors. This preliminary study, which monitored DiD signal in the mice with an IVIS system over a period of 24 h following tail vein injection of the treatments, demonstrates that N1-DiD-NPs show a greater overall fluorescence intensity within tumors than IgG-DiD-NPs at all time points (Figure 5a). In addition, the peak intensity in the tumor occurred at 6 h for IgG-DiD-NPs, but at 12 h for N1-DiD-NPs (Figure 5a, representative IVIS images in Figure 5b). These data indicate that Notch-1 antibody functionalization increases both tumor accumulation and retention of NPs following intravenous administration. It should be noted that fluorescence signal was also observed outside the region of interest (ROI) of the tumor, which is likely due to NP accumulation in the liver. However, there is still a distinct signal in the ROI that is greater for the N1-DiD-NP group than for the IgG-DiD-NP group, suggesting the Notch-1 antibodies improve tumor delivery.

N1-ABT-NPs Reduce Tumor Burden and Extend Survival *in Vivo*.

We then evaluated whether N1-ABT-NPs could reduce tumor volume in a subcutaneous xenograft model. In a preliminary study to investigate the dosing regimen, 18 mice were divided into three groups of six that were treated with saline, IgG-ABT-NPs, or N1-ABT-NPs. The mice were injected with saline or an equivalent volume of NPs at a dose of 10 mg ABT-737/kg once per week for 3 weeks, beginning when tumors were 5 mm in diameter. Tumor volume was measured three times per week, and the average percent change in tumor volume within each treatment group over 1 and 3 weeks is shown in Figure 5c. Tumors in mice treated with N1-ABT-NPs shrank by 37% within 1 week, and after 3 weeks, this reduction in tumor volume was maintained at 44%. By comparison, tumor volume in mice treated with IgG-ABT-NPs and saline increased by 16% and 36%, respectively, within 1 week. By 3 weeks, the mean tumor volumes in the IgG-ABT-NP and saline treatment groups had grown by 65% and 58%, respectively (Figure 5c). These data prompted us to perform a larger follow-up study in which treatments were administered twice per week.

In the subsequent therapeutic study, 24 tumor-bearing mice were divided into three groups of eight that were treated with saline, IgG-ABT-NPs, or N1-ABT-NPs. Over a 55 day treatment period, the mice received intravenous injections of the treatments at a dose of 10 mg of ABT-737/kg twice per week (days indicated by black arrows in Figure 5d), and tumor diameter was measured three times per week (Figure S3). Mice were euthanized when tumors reached 10 mm in diameter, when body weight decreased by more than 20%, or when the study ended at day 55 (whichever came first). The Kaplan–Meier survival curves and average tumor diameter for each group during the treatment period are shown in Figure 5d and Figure S3, respectively. At the end of the study, N1-ABT-NP treated mice exhibited

an 88.9% survival rate, which was substantially improved over the 46.9% and 44.4% survival in the IgG-ABT-NP and saline treated groups, respectively (Figure 5d). We also evaluated the impact of each treatment on mouse weight throughout the therapeutic study (Figure S4a) and on the morphology of major organs at the conclusion of the study using H&E staining (Figure S4b). Mice treated with N1-ABT-NPs did not experience any significant change in body weight or any notable changes in tissue morphology compared to saline treated mice. In contrast, two mice treated with IgG-ABT-NPs demonstrated adverse effects and were euthanized due to severe weight loss or a distended abdomen caused by an enlarged liver and spleen. These data demonstrate that providing targeted delivery of ABT-737 to TNBC tumors, such as *via* Notch-1 antibody functionalized NPs, is important to minimize its adverse effects. Overall, our *in vivo* studies indicate that N1-ABT-NPs are exciting tools for targeted inhibition of Bcl-2 and Notch signaling in TNBC cells that can effectively reduce tumor burden in mice with minimal side effects.

CONCLUSIONS

In this work, we present ABT-737-loaded, Notch-1 antibody functionalized PLGA NPs as potent regulators of Bcl-2 and Notch signaling that can effectively treat TNBC. These N1-ABT-NPs preferentially interact with TNBC cells that overexpress Notch-1 receptors *in vitro*, reducing cell viability and proliferation by molecular mechanisms including inhibition of Bcl-2, suppression of Hes5, HeyL, and Hes1, and amplification of Noxa. *In vivo*, N1-ABT-NPs exhibit enhanced accumulation in subcutaneous TNBC tumors *versus* non-targeted NPs and yield improved tumor growth inhibition and extended animal survival while minimizing adverse effects. With additional development, these N1-ABT-NPs may be a promising arsenal in the fight against TNBC.

Future studies that build on this work should first optimize the NP formulation. While the initial encapsulation efficiency of ABT-737 in unfunctionalized NPs is high (over 95%), there is significant loss of the drug during antibody conjugation. This may be due to drug that is adsorbed onto the surface of the particles rather than physically encapsulated within them. In the future, this loss should be minimized to maximize drug loading and thereby efficacy of the NPs. Additionally, the density of antibodies on the surface of the NPs should be adjusted to yield the loading that provides the greatest specificity and preferential uptake in TNBC cells as well as the greatest inhibition of Notch signaling targets. Finally, for better translation of these NPs into preclinical and clinical tests, the synthesis procedure should be altered to facilitate NP lyophilization and sterilization in powder form prior to administration. Overall, by increasing drug and antibody loading within the NPs, it is expected that tumor inhibition will be enhanced.

Future work that evaluates N1-ABT-NPs should also more extensively examine these NPs' biodistribution, biocompatibility, and efficacy, particularly in mice with an intact immune system. In this study, we used human MDA-MB-231 cells to induce subcutaneous tumors in nude mice, but other TNBC models may more accurately reflect the potential impact of these NPs in humans. It will be important to consider, however, that alternate TNBC models, like murine 4T1 cells, may have varying expression levels of Notch-1 receptors and ligands that will impact the NP-cell interactions and effects.[29] Besides examining different TNBC

cell lines, researchers should also study the effectiveness of N1-ABT-NPs when tumors are positioned orthotopically rather than subcutaneously, as tumor location in the body may impact NP accumulation and retention. When evaluating the biodistribution of these NPs, further steps should also be taken to examine tumors and other major organs *ex vivo*. In this work, live animal imaging revealed fluorescence in an area that was larger than the tumor ROI, likely due to NPs located in the liver. While there is still a distinct signal in the ROI that preliminarily indicates there is enhanced tumor accumulation and retention with Notch-1 functionalized NPs *versus* IgG functionalized NPs, this should be corroborated in future studies by examining tissues *ex vivo* to remove interference from other organs.

While there is evidence showing that Notch-1 is widely overexpressed across human TNBC and correlates with poor prognosis,[30,31] it is classically considered to play the largest role in early stages of tumor development and in cancer stem cells.[32,33] Sethi and Kang have expanded upon this role and demonstrated that Notch signaling facilitates bone metastasis in later stages of tumor progression,[33] but its role in the primary tumor at these later stages has not been extensively explored. In this work, we evaluated the impact of N1-ABT-NPs on tumors in a relatively early stage, about 5 mm in diameter. Future studies should examine the expression of the Notch-1 receptor in tumors of various sizes and determine the biodistribution and therapeutic efficacy of these NPs when treatment is initiated at later stages. Further, the dosing regimen (*e.g.*, NP concentration, number and timing of injections) should be optimized for the treatment of both early and late stage tumors to maximize tumor regression and survival time and realize the full potential of N1-ABT-NPs as anti-TNBC therapeutics.

Besides optimizing the dosing regimen, future studies should directly compare N1-ABT-NPs to freely delivered components *in vivo*. For this work, we did not administer free ABT-737 due to its poor bioavailability and subsequent lack of efficacy.[20,22,36] However, this comparison should be made in future work to confirm that encapsulation in this delivery system is advantageous. It should be noted that, due to ABT-737's lack of solubility, it would need to be delivered orally or intraperitoneally, whereas Notch-1 antibodies would need to be delivered intravenously. As the NPs deliver both agents intravenously, the biodistribution of each agent is likely to be different for free delivery *versus* NP delivery.

In addition to demonstrating the value of N1-ABT-NPs in targeting and regulating the Notch signaling pathway in TNBC, we have also shown that this platform can effectively regulate Bcl-2 through the delivery of ABT-737. Bcl-2 is a promising therapeutic target for many cancers,[34,35] thus extending the potential applicability of this NP formulation. The platform we have developed can be easily adapted to target other cancer types by exchanging the targeting antibody on the surface of the NPs. It is important to consider, however, that not all antibodies are antagonistic. Thus, targeting alternate receptors by exchanging the antibody will not automatically confer the same increase in therapeutic efficacy as was shown here.

Overall, we have demonstrated that ABT-737-loaded, Notch-1 antibody functionalized PLGA NPs can target TNBC cells and effectively regulate Bcl-2 and Notch signaling to induce cell death *in vitro*. In addition, we have shown that these NPs can accumulate in tumors and reduce tumor burden to extend survival in a murine model. These dual antibody/

drug nanocarriers are thus a promising alternative treatment strategy for aggressive cancers like TNBC that are driven by overactive Bcl-2 and Notch signaling. With additional development and implementation, these NPs may substantially improve patient outcomes.

METHODS

Synthesis of N1-ABT-NPs and IgG-ABT-NPs.

ABT-737-loaded PLGA NPs were synthesized using the well-established single emulsion solvent evaporation method.[37] Briefly, PLGA (Lactel, 50:50 carboxylic acid terminated, 39.5 kDa) was dissolved in acetone (VWR) at 1 mg/mL. ABT-737 (Selleckchem, stored in dimethyl sulfoxide (DMSO) at 50 mg/mL) was added to the PLGA in acetone solution at a concentration of 0.05 mg/mL, and this mixture was subsequently added dropwise to distilled water in a 1:3 volume ratio while stirring at 600 rpm. This emulsion continued to stir for 2 h, letting the acetone evaporate. The NPs were then purified using centrifugal filtration (Millipore, 10k MWCO, 4200 g, 30 min) to remove unencapsulated ABT-737 and excess solvent. Rabbit anti-human IgG or Notch-1 antibodies were then conjugated to the surface of the NPs using 1-ethyl-3-(3-dimethylaminopropyl)-carbodiimide (EDC) chemistry.[37,38] Briefly, after centrifugal filtration, ABT-737-loaded NPs were suspended in 4 mM EDC and 4 mM *n*-hydroxysulfosuccinimide sodium salt (sulfo-NHS) and incubated on a rocker (50 rpm) at 4 °C. IgG or Notch-1 antibodies were then added to the solution for further incubation at 4 °C. To remove free antibodies from solution after conjugation, the NPs were purified using trans-flow filtration (Spectrum, 300 kDa MWCO). NPs were freshly prepared and used immediately for experiments. Prior to *in vivo* injections, NPs were washed and suspended in sterile saline.

Characterization of Antibody and Drug Loading in N1-ABT-NPs and Release of ABT-737.

Purified NPs were characterized by DLS and ζ potential measurements on a Litesizer500 instrument (AntonPaar) before and after antibody conjugation, and the reported intensity-based hydrodynamic diameter is the average of three measurements. ABT-737 encapsulation and release were quantified by measuring the absorbance at 300 nm on a Synergy H1 plate reader (BioTek). During NP synthesis, all filtrate containing unencapsulated ABT-737 was collected and lyophilized, then suspended in water, and the absorbance readings were compared to a standard curve of known ABT-737 concentration. To evaluate the release of ABT-737 in storage (water at 4 °C) and physiological (PBS at 37 °C) conditions, NPs were suspended in their respective solvents after antibody conjugation, incubated on an orbital shaker (100 rpm, 37 °C) or rocker (50 rpm, 4 °C), and subsequently centrifuge filtered (4200 rpm, 30 min) at 4, 8, 24, 48, and 72 h to remove released ABT-737. All filtrates were lyophilized, and ABT-737 concentration quantified as described above. To further evaluate the serum stability of N1-ABT-NPs, the NPs were suspended in 0%, 10%, 50%, or 100% FBS diluted in PBS for 2, 6, 12, or 24 h at 37 °C with gentle shaking (100 rpm). DLS and ζ potential measurements were taken at each time point, and the reported hydrodynamic diameter and surface charge are the average of three measurements.

Antibody loading on the NPs was quantified using a solution-based ELISA modified from a previously published protocol.[39] IgG-ABT-NPs, N1-ABT-NPs, or ABT-NPs were incubated

with 10 μg/mL horseradish peroxidase (HRP)-conjugated anti-rabbit IgG antibodies for 1 h at room temperature. Unbound secondary antibodies were removed through centrifugation and the samples were suspended in 3% bovine serum albumin in PBS. The samples were then developed in 3,3',5,5'-tetramethylbenzidine solution (TMB, Sigma-Aldrich) for 10 min before the reaction was stopped with 2 mM sulfuric acid. The absorbance was then measured at 450 nm on a Synergy H1 plate reader and compared to a standard curve of known HRP concentration to calculate the quantity of IgG or Notch-1 antibodies conjugated on 1 mg of PLGA.

Cell Culture.

MDA-MB-231 TNBC cells (American Type Culture Collection, ATCC) were cultured in Dulbecco's modified Eagle's medium (DMEM, VWR) supplemented with 10% FBS (Gemini Bio Products) and 1% penicillin-streptomycin (pen-strep; VWR). MCF-10A cells (ATCC) were cultured in DMEM supplemented with 1% pen-strep, 5% FBS, 50 μg/mL bovine pituitary extract (Sigma), 0.5 μg/mL hydrocortisone (Sigma), 20 ng/mL human epidermal growth factor (StemCell Tech), 10 μg/mL insulin (ThermoFisher), and 100 ng/mL cholera toxin (Sigma). The cultures were maintained at 37 °C in a 5% CO_2 humidified environment. When cells reached 80–90% confluency in T75 cell culture flasks, they were passaged or plated by detaching the cells from the flask using Trypsin-EDTA (Thermo-Fisher) and then counting cells with a hemocytometer.

Evaluating Notch-1 Expression in MDA-MB-231 and MCF-10A Cells.

Notch-1 receptor expression in MDA-MB-231 TNBC cells and MCF-10A breast epithelial cells was analyzed using immunocytochemistry staining. Cells were plated at 2.5×10^4 cells per well (MDA-MB-231 cells) or 1.0×10^4 cells per well (MCF-10A cells) in a 24-well plate and incubated for approximately 48 h. The cells were then fixed in 4% formaldehyde prior to quenching peroxidase reactions with 3% peroxide. The samples were then rinsed with PBS and blocked with 3% bovine serum albumin in PBS for 1 h. After blocking, the cells were then rinsed and incubated in primary anti-human Notch-1 antibody (Santa Cruz; 1 μg/mL) for 1 h at room temperature. The samples were subsequently rinsed three times in PBS and incubated in secondary HRP-conjugated goat anti-rabbit IgG antibody (Pierce; 0.8 μg/mL) for 40 min at room temperature. The cells were rinsed three times in PBS and developed in 3-amino-9-ethylcarbazole (AEC) for 15 min. Finally, the cells were rinsed in PBS and imaged on a Zeiss Axioobserver Z1 Inverted Fluorescence Microscope.

Cellular Binding and Uptake of DiD-Loaded NPs.

To analyze cellular binding and uptake of antibody-functionalized particles, PLGA NPs were loaded with DiD fluorophores (Fisher Scientific; excitation 644 nm/emission 665 nm) instead of ABT-737 and functionalized as described above to create IgG-DiD-NPs and N1-DiD-NPs. For image-based analysis, cells were plated at 6×10^4 cells per well (MDA-MB-231 cells) or 2.5×10^4 cells per well (MCF-10A cells) in an 8-well Lab-Tek II chamber slide and incubated overnight. Cells were then treated with IgG-DiD-NPs and N1-DiD-NPs at 80 nM DiD or were left untreated and incubated for 4 h. After 4 h, the cells were rinsed with PBS to remove unbound NPs, fixed in 4% formaldehyde, and permeabilized with 0.5% Triton X-100 in PBS with 5% bovine serum albumin. The cells were then counterstained

with DyLight 554-Phalloidin (Cell Signaling Technology) overnight at 4 °C. The slides were mounted in ProLong Gold Antifade with DAPI (Vectashield) and imaged on an Axioobserver Z1 Inverted Fluorescence Microscope (Zeiss).

For flow cytometric analysis of cellular binding and uptake, cells were plated at 3×10^4 cells per well (MDA-MB-231 cells) or 2×10^4 cells per well (MCF-10A cells) in a 24-well plate and incubated overnight. Cells were then treated with IgG-DiD-NPs and N1-DiD-NPs at 50 nM DiD or were left untreated and incubated for 0, 1, 4, 8, 12, 16, or 24 h prior to rinsing with PBS. The cells were then lifted off the plate with Trypsin-EDTA and resuspended in PBS to yield a cell suspension. All cell suspensions were analyzed using an Acea Novocyte 2060 flow cytometer with the APC (excitation, 640 nm; emission, 675/30 nm) channel. Density plots showing forward and side scatter data were used to create a primary gate for cells, excluding debris, prior to analyzing DiD content. Flow cytometric analysis was performed in triplicate.

Effect of Free Components and NPs on Metabolic Activity.

To evaluate the toxicity of freely delivered ABT-737 and IgG or Notch-1 antibodies *versus* nanocarriers (*i.e.*, IgG-ABT-NPs and N1-ABT-NPs) using a MTT assay, MDA-MB-231 cells were plated at 5×10^3 cells per well in a 96-well plate and incubated overnight. Cells were treated with 0, 1, 2, 3, 4, or 5 μM ABT-737 and 0, 0.3, 0.6, 0.9,1.2, or 1.5 μg/mL IgG or Notch-1 antibody, either freely in solution or in NP form for 72 h. After 72 h, the treatments were removed, and the cells were incubated in MTT solution per the manufacturer's instructions (ThermoFisher). After 3 h, the MTT solution was replaced with DMSO, and the absorbance at 540 nm was read on a Synergy H1 plate reader (BioTek). To analyze the data, background (DMSO in wells without cells) was subtracted from the absorbance reading in each well. Triplicate well signals were averaged and then normalized to untreated cells. These experiments were performed in triplicate, and data were analyzed by one-way ANOVA with post hoc Tukey.

Analyzing the Effect of N1-ABT-NPs or IgG-ABT-NPs on Cell Proliferation.

To analyze the effect of IgG-ABT-NPs and N1-ABT-NPs on cellular proliferation *via* an EdU assay, cells were seeded at 1.0×10^5 cells per well in a 12-well plate and incubated overnight. Cells were then treated with IgG-ABT-NPs or N1-ABT-NPs at 3 μM ABT-737 for 72 h. Sixteen hours prior to the end of the treatment period, cells were spiked with EdU at 10 μM. Cells were then prepared per the manufacturer's instructions modified for a single cell suspension. Briefly, cells were fixed in 4% formaldehyde and permeabilized with0.5% Triton X-100. They were subsequently incubated in the Click-iT reaction cocktail, washed in PBS, and examined on an Acea Novocyte 2060 flow cytometer with the FITC (excitation, 488 nm; emission, 530/30 nm) channel. Density plots showing forward and side scatter data were used to create a primary gate for cells, excluding debris, prior to analyzing EdU-labeling azide content. Flow cytometric analysis was performed in quadruplicate, and statistical analysis was performed using a one-way ANOVA with post hoc Tukey.

Evaluating Changes in Gene Expression Induced by N1-ABT-NPs.

To determine the effects of IgG-ABT-NPs and N1-ABT-NPs on gene expression in TNBC cells by quantitative real-time polymerase chain reaction (qRT-PCR), MDA-MB-231 cells were seeded at 1.5×10^5 cells per well in a 6-well plate and incubated overnight. Cells were then treated with IgG-ABT-NPs or N1-ABT-NPs at 3 μM ABT-737 for 72 h. At the conclusion of the treatment period, cells were rinsed with PBS, and mRNA was extracted using a Bioline Isolate II RNA Mini Kit. qRT-PCR was then performed using SensiFAST SYBR One-Step Master Mix on a LightCycler 96 (Roche). and gene expression was normalized to that of RPLPO. These experiments were performed in triplicate and analyzed using a one-way ANOVA with post hoc Tukey. Primer sequences are listed in Table S1.

Investigating Changes in Protein Expression Induced by N1-ABT-NPs.

To further evaluate the effects of N1-ABT-NPs on Bcl-2 and Notch signaling targets by Western blotting, MDA-MB-231 cells were plated at 1.5×10^5 cells per well in a 6-well plate and incubated overnight. Cells were then treated as described for qRT-PCR. After 72 h of treatment with IgG-ABT-NPs or N1-ABT-NPs, the cells were rinsed with PBS and lysed in RIPA buffer supplemented with Halt Protease Inhibitor in a 1:50 volume ratio. After removing membrane debris through centrifugation, the extracted protein was quantified using a DC Protein Assay (BioRad), and 10 μg of protein was separated on 4–12% bis-tris gels at 135 V for 60 min. Then, the protein was transferred to a 0.2 μm nitrocellulose membrane for 10 min using a Power Blotter System (Invitrogen). The membrane was subsequently blocked for 60 min in 5% milk in tris buffered saline with 0.1% Tween-20 (TBS-T) and then incubated with rabbit anti-human Bcl-2 (ProteinTech; 1:1000), cleaved Notch-1 (Cell Signaling Technology; 1:250), and Hes1 antibodies (Cell Signaling Technology; 1:500) in 5% milk in TBS-T overnight at 4 °C. Mouse anti-human β-actin antibody (Cell Signaling Technology; 1:20,000) was used as the normalization control. After incubation in primary antibodies, membranes were washed 3× in TBS-T and incubated with HRP-anti-rabbit or mouse IgG antibody (VWR; 1:25,000) in 5% milk in TBS-T for 1 h at room temperature. Membranes were then washed 2× in TBS-T and 2× in TBS (without Tween-20), and protein bands were visualized using a Pierce enhanced chemiluminescence detection solution (ECL, Thermo Scientific). Band densities were quantified in ImageJ, and Bcl-2, cleaved Notch-1, and Hes1 densities were normalized to that of β-actin prior to further normalizing treatment groups to the control untreated group. The data shown represent the average band density across three trials and were analyzed using a one-way ANOVA with post hoc Tukey.

In Vivo Tumor Model.

Female nude mice around 5 weeks old were purchased from Charles River Laboratories. The Institutional Animal Care and Use Committee (IACUC) of the University of Delaware approved all procedures. MDA-MB-231 cells in matrigel (1×10^6 cells per 100 μL) were administered subcutaneously into the right flank of the mice, and tumor growth was monitored at least 3× per week afterward with Vernier calipers. Treatments for three separate studies were administered intravenously when tumors reached 5 mm in diameter. A preliminary biodistribution study utilized 6 mice per treatment group (saline, IgG-DiD-NPs,

N1-DiD-NPs), a dose optimization study utilized 6 mice per treatment group (saline, IgG-ABT-NPs, N1-ABT-NPs), and a larger therapeutic study utilized 8 mice per treatment group (saline, IgG-ABT-NPs, N1-ABT-NPs). Details of these studies are provided in the following sections.

Assessment of NP Biodistribution *in Vivo* Following Tail Vein Administration.

To reveal the time of maximum NP accumulation within tumors following intravenous administration, mice were injected with 100 μL saline or with IgG-DiD-NPs or N1-DiD-NPs at a concentration of 50 μM DiD. These mice were imaged under isoflurane anesthesia with an IVIS Lumina Imaging System (PerkinElmer) immediately, 6, 12, and 24 h after injection to monitor DiD signal in the tumors *versus* time using the Cy5.5 (excitation, 678 nm; emission, 694 nm) channel. The fluorescence intensity within the tumors at each time point was measured in ImageJ software after drawing a ROI around the tumor, and the mean intensity at each time point was calculated.

Evaluating the Effect of N1-ABT-NPs on Tumor Growth *in Vivo*.

Mice were injected with saline or with IgG-ABT-NPs or N1-ABT-NPs at doses of 10 mg ABT-737/kg when tumors reached 5 mm in diameter (day 0) for a dose optimization and full study, as described above. For the dose optimization study, mice received two subsequent injections on days 7 and 14 for a total of three treatments. The tumor length and width in each mouse were measured with Vernier calipers 3× per week until day 21, and tumor volume was calculated as (tumor length) × (tumor width)^2/2. These data were used to calculate the mean tumor volume in each group and the relative tumor volume compared to day 0. On day 21, the mice were euthanized. Statistical analysis was performed on the average percent change in tumor volume using a one-way ANOVA with post hoc Tukey.

For the full therapeutic study in which treatment was performed twice per week, mice were injected as stated above on day 0 and received seven subsequent injections on days 4, 7, 11, 14, 18, 21, and 25 for a total of eight treatments. The tumor length and width in each mouse were measured with Vernier calipers 3× per week until day 55, and tumor volume was calculated as above. Mice were euthanized upon >20% loss in weight, when tumors reached 10 mm in diameter, or on day 55, whichever came first. These data were used to create the presented Kaplan–Meier survival curves, and statistical significance was examined using a log-rank test.

Upon euthanasia, the major organs (spleen, liver, kidneys, heart, GI tract, lungs, and brain) of the mice used in the full therapeutic study were excised for histological analysis by hematoxylin and eosin (H&E) staining. The excised tissues were placed into embedding cassettes, rinsed once in 1× PBS, and then fixed in 4% paraformaldehyde at 4 °C for 72 h. The tissues were then rinsed 3 times in 70% ethanol for 10 min each and stored in 70% ethanol until processing. The fixed tissues were processed and embedded with paraffin. Embedded tissues were cut into 5 μm slices and stained with H&E to enable visualization of tissue structure. Briefly, the tissues were deparaffinized with xylene and rehydrated prior to hematoxylin staining and subsequent counterstaining with eosin. After staining, the tissues were dehydrated and mounted for imaging with a xylene-based mounting medium. H&E

stained tissues were imaged on an Axioobserver Z1 Inverted Fluorescence Microscope (Zeiss).

Supplementary Material

Refer to Web version on PubMed Central for supplementary material.

ACKNOWLEDGMENTS

This research was supported by the National Institute of General Medical Sciences of the National Institutes of Health under award number R35GM119659. We thank E. Pappas for her assistance with the histological processing of excised organs from our *in vivo* studies.

REFERENCES

(1). Bianchini G; Balko JM; Mayer IA; Sanders ME; Gianni L Triple-Negative Breast Cancer: Challenges and Opportunities of a Heterogeneous Disease. Nat. Rev. Clin. Oncol 2016, 13, 674–690. [PubMed: 27184417]

(2). Turner N; Moretti E; Siclari O; Migliaccio I; Santarpia L; D'Incalci M; Piccolo S; Veronesi A; Zambelli A; Del Sal G; Di Leo A Targeting Triple Negative Breast Cancer: Is p53 the Answer? Cancer Treat. Rev 2013, 39, 541–550. [PubMed: 23321033]

(3). Griffiths CL; Olin JL Triple Negative Breast Cancer: A Brief Review of Its Characteristics and Treatment Options. J. Pharm. Pract 2012, 25, 319–323. [PubMed: 22551559]

(4). Ahmad A; Banerjee S; Wang Z; Kong D; Sarkar FH Plumbagin-Induced Apoptosis of Human Breast Cancer Cells Is Mediated by Inactivation of NF-KB and Bcl-2. J. Cell. Biochem 2008, 105, 1461–1471. [PubMed: 18980240]

(5). Mungamuri SK; Yang X; Thor AD; Somasundaram K Survival Signaling by Notch1: Mammalian Target of Rapamycin (mTOR)-Dependent Inhibition of p53. Cancer Res. 2006, 66, 4715–4725. [PubMed: 16651424]

(6). Inao T; Iida Y; Moritani T; Okimoto T; Tanino R; Kotani H; Harada M Bcl-2 Inhibition Sensitizes Triple-Negative Human Breast Cancer Cells to Doxorubicin. Oncotarget 2018, 9, 25545–25556. [PubMed: 29876007]

(7). Yuan Z; Jiang H; Zhu X; Liu X; Li J Ginsenoside Rg3 Promotes Cytotoxicity of Paclitaxel through Inhibiting NF-kB Signaling and Regulating Bax/Bcl-2 Expression on Triple-Negative Breast Cancer. Biomed. Pharmacother 2017, 89, 227–232. [PubMed: 28231544]

(8). Speiser J; Foreman K; Drinka E; Godellas C; Perez C; Salhadar A; Ersahin C; Rajan P Notch-1 and Notch-4 Biomarker Expression in Triple-Negative Breast Cancer. Int. J. Surg. Pathol 2012, 20, 137–143.

(9). Haupt S; Berger M; Goldberg Z; Haupt Y Apoptosis - The p53 Network. J. Cell Sci 2003, 116, 4077–4085. [PubMed: 12972501]

(10). Deng X; Cao M; Zhang J; Hu K; Yin Z; Zhou Z; Xiao X; Yang Y; Sheng W; Wu Y; Zeng Y Hyaluronic Acid-Chitosan Nanoparticles for Co-Delivery of MiR-34a and Doxorubicin in Therapy against Triple Negative Breast Cancer. Biomaterials 2014, 35, 4333–4344. [PubMed: 24565525]

(11). Ozretic P; Alvir I; Sarcevic B; Vujaskovic Z; Rendic-Miocevic Z; Roguljic A; Beketic-Oreskovic L Apoptosis Regulator Bcl-2 Is an Independent Prognostic Marker for Worse Overall Survival in Triple-Negative Breast Cancer Patients. Int. J. Biol. Markers 2018, 33, 109–115. [PubMed: 28777433]

(12). Adams JM; Cory S The Bcl-2 Apoptotic Switch in Cancer Development and Therapy. Oncogene 2007, 26, 1324–1337. [PubMed: 17322918]

(13). Rooswinkel R; van de Kooij B; Verheij M; Borst J Bcl-2 Is a Better ABT-737 Target than Bcl-xL or Bcl-W and Only Noxa Overcomes Resistance Mediated by Mcl-1, Bfl-1, or Bcl-B. Cell Death Dis. 2012, 3, 366.

(14). Billard C BH3Mimetics: Status of the Field and New Developments. Mol. Cancer Ther 2013, 12, 1691–1701. [PubMed: 23974697]

(15). Sakakibara-Konishi J; Ikezawa Y; Oizumi S; Kikuchi J; Kikuchi E; Mizugaki H; Kinoshita I; Dosaka-Akita H; Nishimura M Combined Antitumor Effect of γ-Secretase Inhibitor and ABT-737 in Notch-Expressing Non-Small Cell Lung Cancer. Int. J. Clin. Oncol 2017, 22, 257–268. [PubMed: 27816990]

(16). Schmid D; Jarvis GE; Fay F; Small DM; Greene MK; Majkut J; Spence S; Mclaughlin KM; Mccloskey KD; Johnston PG; Kissenpfennig A; Longley DB; Scott CJ Nano-encapsulation of ABT-737 and Camptothecin Enhances Their Clinical Potential through Synergistic Antitumor Effects and Reduction of Systemic Toxicity. Cell Death Dis. 2014, 5, 1454.

(17). Séveno C; Loussouarn D; Bréchet S; Campone M; Juin P; Barillé-Nion S Gamma-Secretase Inhibition Promotes Cell Death, Noxa Upregulation, and Sensitization to BH3Mimetic ABT-737 in Human Breast Cancer Cells. Breast Cancer Res. 2012, 14, R96. [PubMed: 22703841]

(18). Park C; Bruncko M; Adickes J; Bauch J; Ding H; Kunzer A; Marsh KC; Nimmer P; Shoemaker AR; Song X; Tahir SK; Tse C; Wang X; Wendt MD; Yang X; Zhang H; Fesik SW; Rosenberg SH; Elmore SW Discovery of an Orally Bioavailable Small Molecule Inhibitor of Prosurvival B-Cell Lymphoma 2 Proteins. J. Med. Chem 2008, 51, 6902–6915. [PubMed: 18841882]

(19). Gandhi L; Camidge DR; de Oliveira MR; Bonomi P; Gandara D; Khaira D; Hann CL; Mckeegan EM; Litvinovich E; Hemken PM; Dive C; Enschede SH; Nolan C; Chiu Y-L; Busman T; Xiong H; Krivoshik AP; Humerickhouse R; Shapiro GI; Rudin CM Phase I Study of Navitoclax (ABT-263), a Novel Bcl-2 Family Inhibitor, in Patients with Small-Cell Lung Cancer and Other Solid Tumors. J. Clin. Oncol 2011, 29, 909–916. [PubMed: 21282543]

(20). Wilson WH; O'Connor OA; Czuczman MS; LaCasce AS; Gerecitano JF; Leonard JP; Tulpule A; Dunleavy K; Xiong H; Chiu Y-L; Cui Y; Busman T; Elmore SW; Rosenberg SH; Krivoshik AP; Enschede SH; Humerickhouse RA Safety, Pharmacokinetics, Pharmacodynamics, and Activity of Navitoclax, a Targeted High Affinity Inhibitor of BCL-2, in Lymphoid Malig-nancies. Lancet Oncol. 2010, 11, 1149–1159. [PubMed: 21094089]

(21). Rudin CM; Hann CL; Garon EB; de Oliveira MR; Bonomi PD; Camidge DR; Chu Q; Giaccone G; Khaira D; Ramalingam SS; Ranson MR; Dive C; McKeegan EM; Chyla BJ; Dowell BL; Chakravartty A; Nolan CE; Rudersdorf N; Busman TA; Mabry MH; et al. Phase II Study of Single-Agent Navitoclax (ABT-263) and Biomarker Correlates in Patients with Relapsed Small Cell Lung Cancer. Clin. Cancer Res 2012, 18, 3163–3169. [PubMed: 22496272]

(22). Wu X; Wang L; Qiu Y; Zhang B; Hu Z; Jin R Cooperation of IRAK1/4 Inhibitor and ABT-737 in Nanoparticles for Synergistic Therapy of T Cell Acute Lymphoblastic Leukemia. Int. J. Nanomed 2017, 12, 8025–8034.

(23). Nickoloff BJ; Hendrix ÃMJC; Pollock PM; Trent JM; Miele L; Qin J Notch and NOXA-Related Pathways in Melanoma Cells. J. Invest. Dermatol. Symp. Proc 2005, 10, 95–104.

(24). Valcourt DM; Dang MN; Wang J; Day ES Nanoparticles for Manipulation of the Developmental Wnt, Hedge-hog, and Notch Signaling Pathways in Cancer. Ann. Biomed. Eng 2019, 1–21.

(25). Speiser JJ; Ersahin C; Osipo C The Functional Role of Notch Signaling in Triple-Negative Breast Cancer In Hormones and Breast Cancer: Vitamins and Hormones; Litwack G, Ed.; Academic Press: London, 2013; Vol. 93, pp 277–306.

(26). Valcourt DM; Harris J; Riley RS; Dang M; Wang J; Day ES Advances in Targeted Nanotherapeutics: From Bioconjugation to Biomimicry. Nano Res. 2018, 11, 4999–5016. [PubMed: 31772723]

(27). Riley RS; Day ES Frizzled7 Antibody-Functionalized Nanoshells Enable Multivalent Binding for Wnt Signaling Inhibition in Triple Negative Breast Cancer Cells. Small 2017, 13, 1700544.

(28). Scott AM; Wolchok JD; Old LJ Antibody Therapy of Cancer. Nat. Rev. Cancer 2012, 12, 278–287. [PubMed: 22437872]

(29). Kumar S; Srivastav RK; Wilkes DW; Ross T; Kim S; Kowalski J; Chatla S; Zhang Q; Nayak A; Guha M; Fuchs SY; Thomas C; Chakrabarti R Estrogen-Dependent DLL1-Mediated Notch Signaling Promotes Luminal Breast Cancer. Oncogene 2019, 38, 2092–2107. [PubMed: 30442981]

(30). Stylianou S; Clarke RB; Brennan K Aberrant Activation of Notch Signaling in Human Breast Cancer. Cancer Res. 2006, 66, 1517–1526. [PubMed: 16452208]

(31). Yuan X; Zhang M; Wu H; Xu H; Han N; Chu Q; Yu S; Chen Y; Wu K Expression of Notch1 Correlates with Breast Cancer Progression and Prognosis. PLoS One 2015, 10, e0131689. [PubMed: 26121683]

(32). Mollen EWJ; Ient J; Tjan-Heijnen VCG; Boersma LJ; Miele L; Smidt ML; Vooijs MA G. G. Moving Breast Cancer Therapy Up a Notch. Front. Oncol 2018, 8, 518. [PubMed: 30515368]

(33). Sethi N; Kang Y Notch Signalling in Cancer Progression and Bone Metastasis. Br. J. Cancer 2011, 105, 1805–1810. [PubMed: 22075946]

(34). Campbell KJ; Tait SWG Targeting BCL-2 Regulated Apoptosis in Cancer. Open Biol. 2018, 8, 180002. [PubMed: 29769323]

(35). Yip KW; Reed JC Bcl-2 Family Proteins and Cancer. Oncogene 2008, 27, 6398–6406. [PubMed: 18955968]

(36). Sivakumar D; Aashis R; Sivaraman T In Silico Rationalization for the Differential Bioavailability of ABT-737 and ABT-263 That Antagonise the Anti-Apoptotic Proteins. Int. J. Pharm. Sci. Res 2011, 3, 1141–1145.

(37). Srinivasan S; Manchanda R; Lei T; Nagesetti A; Fernandez-Fernandez A; Mcgoron AJ Targeted Nanoparticles for Simultaneous Delivery of Chemotherapeutic and Hyperthermia Agents – An *In Vitro* Study. J. Photochem. Photobiol., B 2014, 136, 81–90. [PubMed: 24859437]

(38). Kocbek P; Obermajer N; Cegnar M; Kos J; Kristl J Targeting Cancer Cells Using PLGA Nanoparticles Surface Modified with Monoclonal Antibody. J. Controlled Release 2007, 120, 18–26.

(39). Riley RS; Melamed JR; Day ES Enzyme-Linked Immunosorbent Assay to Quantify Targeting Molecules on Nanoparticles In Targeted Drug Delivery: Methods in Molecular Biology; Sirianni R, Behkam B, Eds.; Humana Press: New York, 2018; Vol. 1831, pp 145–157.

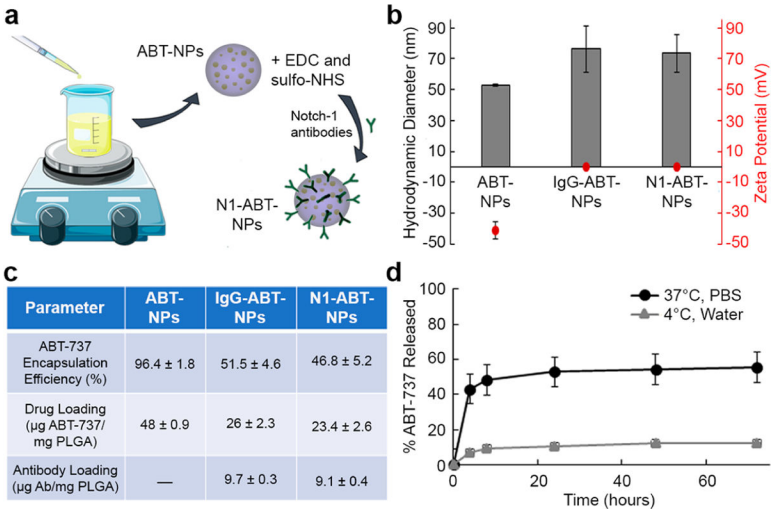

Parameter	ABT-NPs	IgG-ABT-NPs	N1-ABT-NPs
ABT-737 Encapsulation Efficiency (%)	96.4 ± 1.8	51.5 ± 4.6	46.8 ± 5.2
Drug Loading (μg ABT-737/ mg PLGA)	48 ± 0.9	26 ± 2.3	23.4 ± 2.6
Antibody Loading (μg Ab/mg PLGA)	—	9.7 ± 0.3	9.1 ± 0.4

Figure 1.

Synthesis and characterization of N1-ABT-NPs. (a) Scheme depicting N1-ABT-NP synthesis. (b) Hydrodynamic diameter and ζ potential of ABT-737-loaded NPs before and after conjugation with IgG or Notch-1 antibodies. (c) Loading of ABT-737 and antibodies before and after antibody conjugation. (d) ABT-737 release from N1-ABT-NPs in storage (4 °C, water) and physiological (37 °C, PBS) conditions. Portions of this figure were produced with permission using Servier Medical ART templates, which are licensed under a Creative Commons Attribution 3.0 Unported License from Servier Medical Art; https://smart.servier.com.

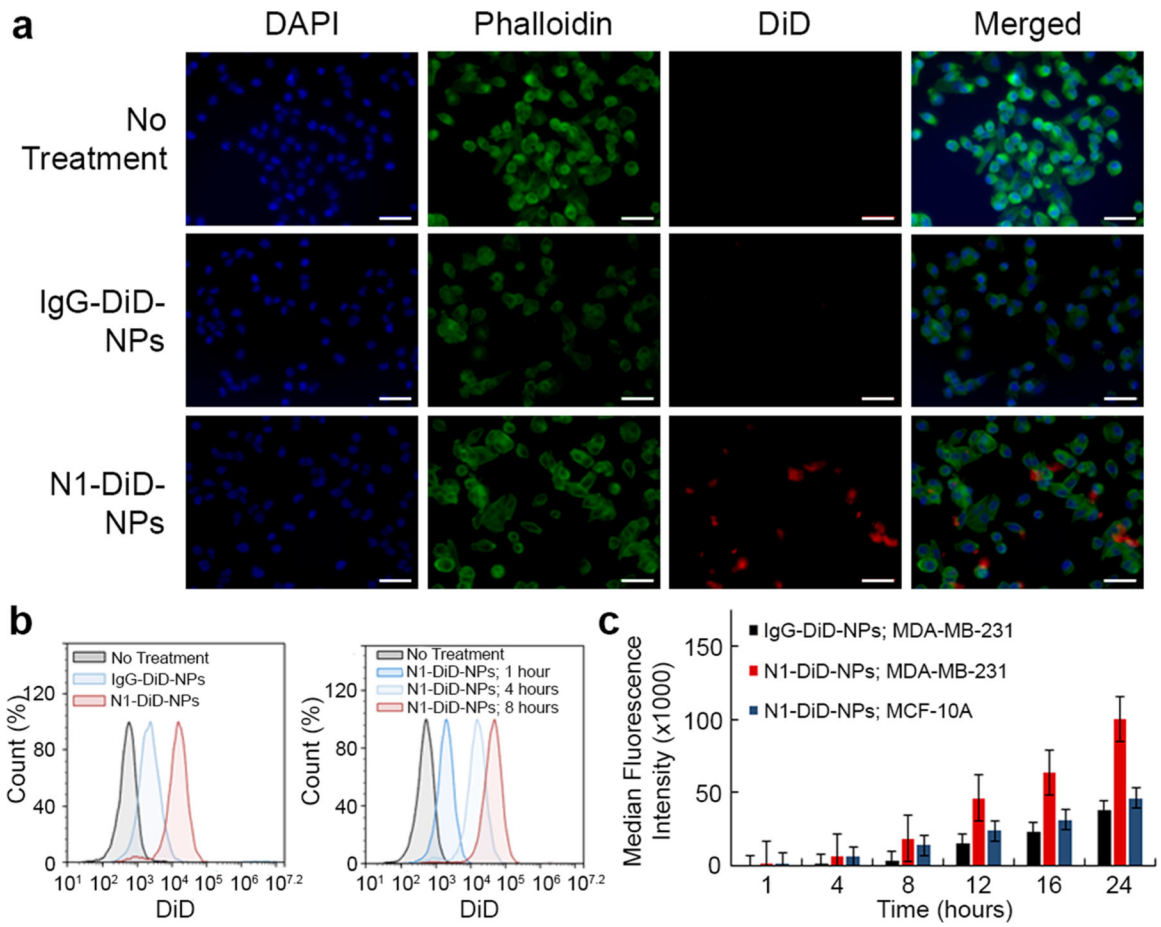

Figure 2.

Analysis of N1-DiD-NPs interaction with TNBC cells *versus* healthy breast epithelial cells. (a) Fluorescence microscopy images showing MDA-MB-231 TNBC cells treated with no NPs, IgG-DiD-NPs, or N1-DiD-NPs. Cell nuclei are blue (DAPI), actin is green (Phalloidin), and NPs are red (DiD). Scale bars = 50 μm. (b) Representative flow cytometry histograms of MDA-MB-231 TNBC cells exposed to IgG-DiD-NPs or N1-DiD-NPs. (c) Median DiD fluorescence intensity of MDA-MB-231 TNBC cells and healthy MCF-10A mammary cells treated with N1-DiD-NPs or IgG-DiD-NPs as measured by flow cytometry (n = 3).

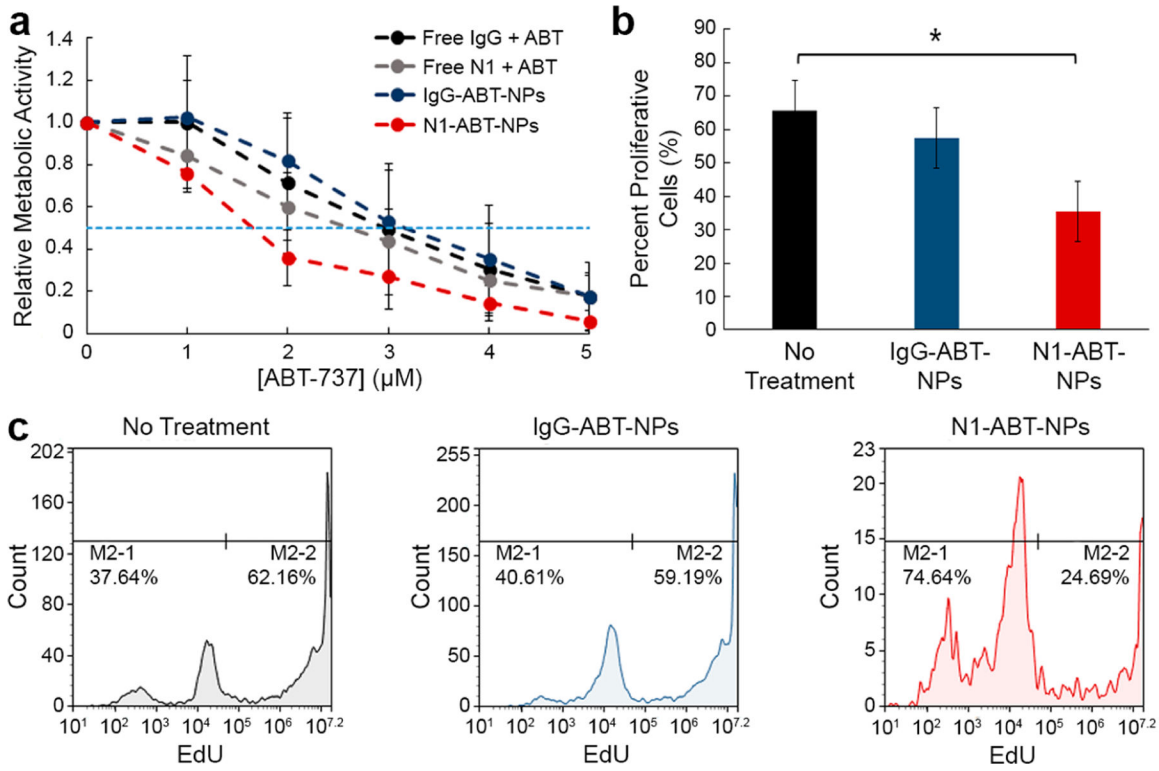

Figure 3.

Analysis of the impact of N1-ABT-NPs on TNBC cell metabolic activity and proliferation. (a) Relative metabolic activity of MDA-MB-231 cells treated with different doses of freely delivered IgG or Notch-1 (N1) antibodies and ABT-737 or with nanocarriers (IgG-ABT-NPs or N1-ABT-NPs) as measured by an MTT assay ($n = 3$). Horizontal dotted line indicates 50% reduction in metabolic activity. (b) Percent proliferation of MDA-MB-231 TNBC cells that were untreated or exposed to IgG-ABT-NPs or N1-ABT-NPs ($n = 4$). *$p < 0.05$ by one-way ANOVA with post hoc Tukey. (c) Representative flow cytometry histograms for EdU proliferation assay.

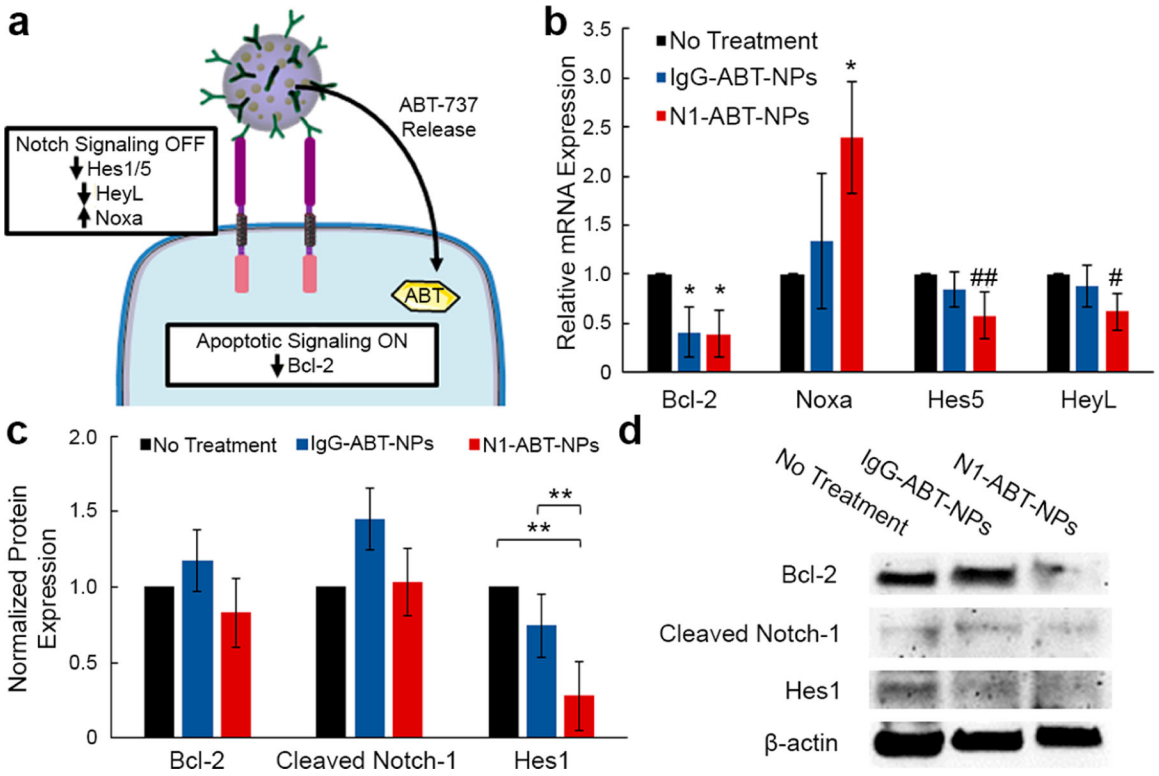

Figure 4.

Examination of the effects of N1-ABT-NPs on Notch signaling and Bcl-2 expression in TNBC cells. (a) Scheme of proposed NP interaction with MDA-MB-231 TNBC cells. Upon cellular binding, N1-ABT-NPs suppress Notch signaling through antibody-mediated signal cascade interference and also release ABT-737 to inhibit Bcl-2 and activate apoptosis. (b) qRT-PCR analysis of relative Bcl-2, Noxa, Hes5, and HeyL mRNA expression after treatment with IgG- or N1-ABT-NPs compared to control (untreated) cells ($n = 3$). RPLPO was used as a control and relative mRNA expression in NP treated groups is normalized to that of untreated cells. *$p < 0.05$, ##$p = 0.06$, #$p = 0.07$ (c) Quazi-quantitative analysis of Western blotting for normalized Bcl-2, cleaved Notch-1, and Hes1 protein expression ($n = 3$). β-actin was used as a control, and expression in NP-treated samples was normalized to expression in untreated cells. **$p < 0.01$. (d) Representative Western blot bands for Bcl-2, cleaved Notch-1, Hes1, and β-actin protein levels. Portions of this figure were produced with permission using Servier Medical ART templates, which are licensed under a Creative Commons Attribution 3.0 Unported License from Servier Medical Art; https://smart.servier.com.

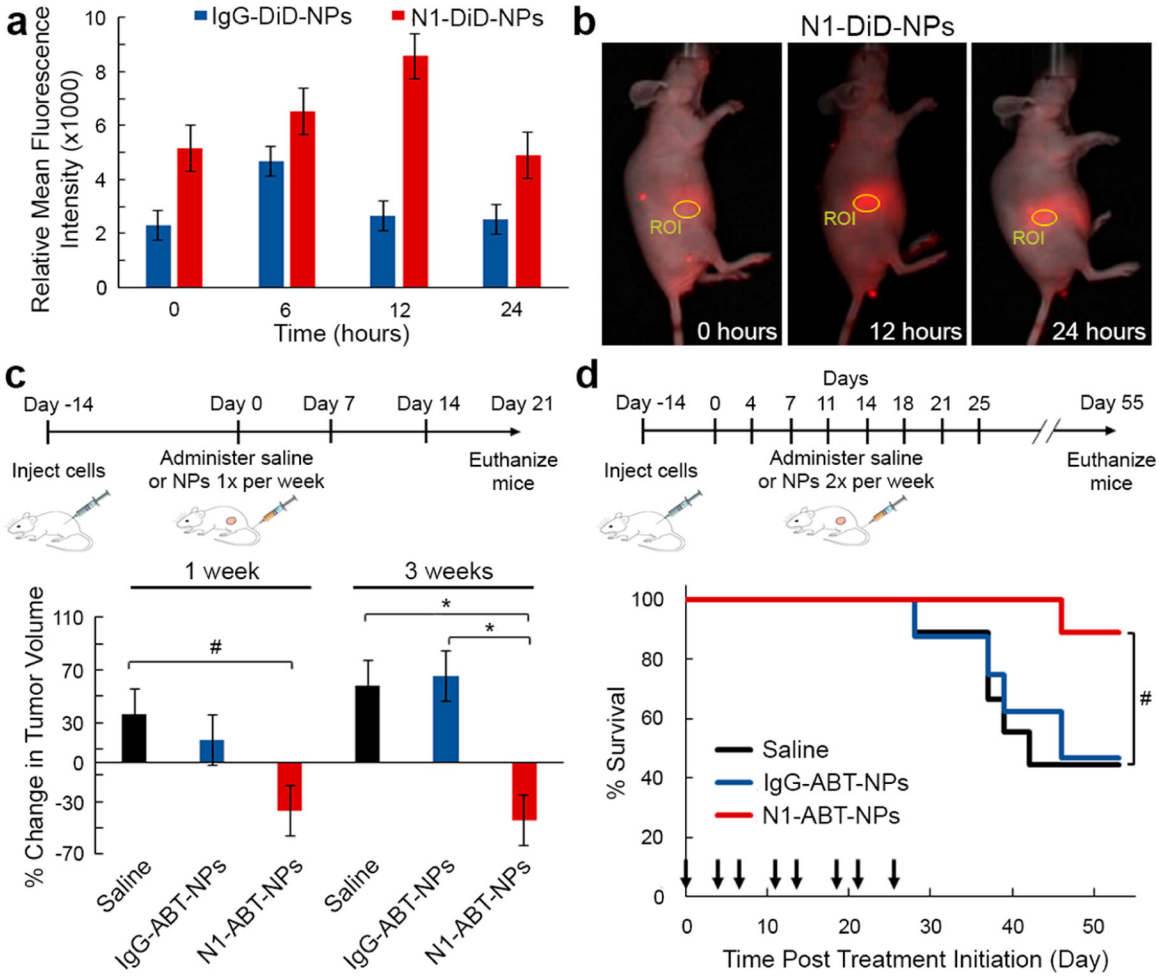

Figure 5.

In vivo evaluation of N1-ABT-NPs as a treatment for TNBC. (a) Relative mean fluorescence intensity of DiD in subcutaneous MDA-MB-231 tumors in mice 0, 6, 12, and 24 h post-intravenous injection of IgG-DiD-NPs or N1-DiD-NPs ($n = 6$). (b) Representative fluorescence images of a mouse treated with N1-DiD-NPs at 0, 12, and 24 h after injection. Circles indicate the region of interest (ROI) where fluorescence intensity was measured. (c) Average percent change in tumor volume ($n = 6$ mice/group) after 1 and 3 weeks of treatment with saline, IgG-ABT-NPs, or N1-ABT-NPs at 10 mg ABT-737/kg once per week. #$p < 0.1$, *$p < 0.05$ by one-way ANOVA with post hoc Tukey. (d) Kaplan–Meier survival curves for mice bearing subcutaneous MDA-MB-231 TNBC tumors that were treated intravenously with saline, IgG-ABT-NPs, or N1-ABT-NPs at 10 mg ABT-737/kg twice per week for 4 weeks. Black arrows on the *x*-axis indicate days of treatment; $n = 8$ mice/group. #$p = 0.10$ by log-rank test. Portions of this figure were produced with permission using Servier Medical ART templates, which are licensed under a Creative Commons Attribution 3.0 Unported License from Servier Medical Art; https://smart.servier.com.

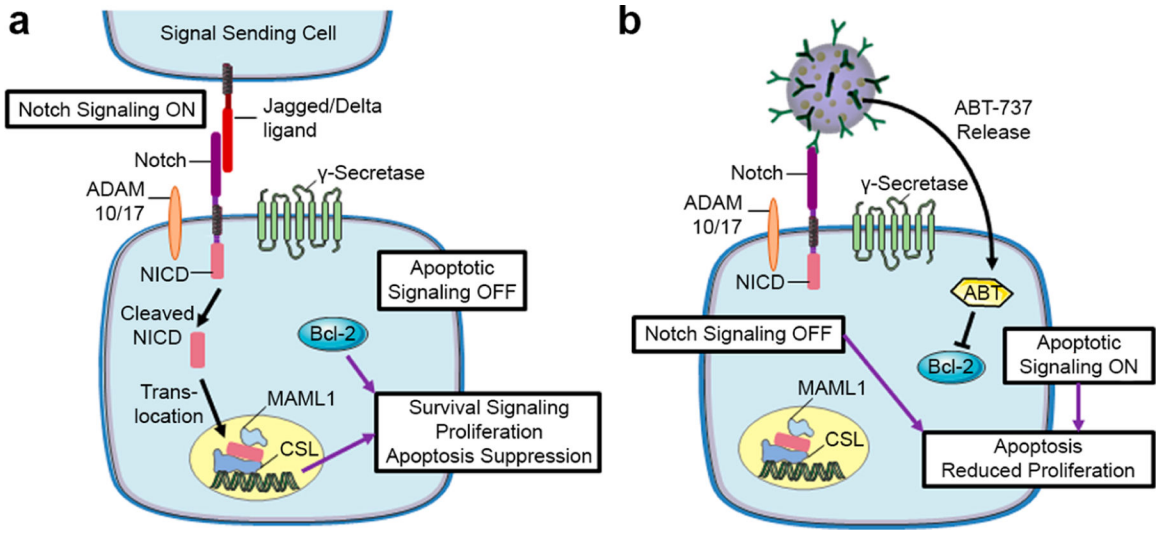

Scheme 1. Depiction of How Notch Signaling and Bcl-2 Contribute to TNBC Progression and How N1-ABT-NPs Could Be Utilized to Inhibit These Pathways and Slow Tumor Growth[a]

[a](a) Notch signaling is activated in TNBC cells when overexpressed Notch-1 receptors interact with Jagged or Delta ligands on neighboring cells. This leads to cleavage of the NICD, which translocates to the nucleus to activate signaling that supports TNBC cell survival, proliferation, and apoptosis suppression. Bcl-2 is an anti-apoptotic protein that is also overexpressed in TNBC and contributes to poor clinical outcomes. (b) Scheme depicting the posited effects of N1-ABT-NPs on TNBC cells. N1-ABT-NPs can bind Notch-1 receptors on TNBC cells to lock them in a ligand unresponsive state, thereby turning off Notch signaling. Simultaneously, these NPs can release the Bcl-2 inhibitor ABT-737. Together, these effects promote apoptosis and reduce cellular proliferation. This figure was produced with permission using Servier Medical ART templates, which are licensed under a Creative Commons Attribution 3.0 Unported License from Servier Medical Art; https://smart.servier.com.